

Low-temperature growth of InAs/GaSb superlattices on miscut GaAs substrates for mid-wave infrared detectors

Piotr Martyniuk^{a*}, Djalal Benyahia^b^a Institute of Applied Physics, Military University of Technology, gen. Sylwestra Kaliskiego 2, 00-908 Warsaw, Poland^b Laboratoire des Systèmes Lasers, École Militaire Polytechnique, BP 17 Bordj El Bahri, 16111 Algiers, Algeria

Article info

Article history:

Received 12 Oct. 2022

Received in revised form 14 Dec. 2022

Accepted 14 Dec. 2022

Available on-line 24 Feb. 2023

Keywords:

Molecular beam epitaxy; superlattice;

X-ray diffraction; III-V semiconductor.

Abstract

Short-period 10 monolayers InAs/10ML GaSb type-II superlattices have been deposited on a highly lattice-mismatched GaAs (001), 2° offcut towards <110> substrates by molecular beam epitaxy. This superlattice was designed for detection in the mid-wave infrared spectral region (cut-off wavelength, $\lambda_{\text{cut-off}} = 5.4 \mu\text{m}$ at 300 K). The growth was performed at relatively low temperatures. The InAs/GaSb superlattices were grown on a GaSb buffer layer by an interfacial misfit array in order to relieve the strain due to the ~7.6% lattice-mismatch between the GaAs substrate and type-II superlattices. The X-ray characterisation reveals a good crystalline quality exhibiting full width at half maximum ~100 arcsec of the zero-order peak. Besides, the grown samples have been found to exhibit a change in the conductivity.

1. Introduction

After the conception of InAs/GaSb type-II superlattices (T2SLs) in 1977, numerous research groups have investigated this semiconductor material [1]. T2SLs infrared (IR) detectors exhibit higher performance than the state-of-the-art materials for the future generation applications [2, 3]. Indeed, the well-known HgCdTe ternary alloy exhibits technological problems, surface and interfaces instabilities, and high dark current which limits the performance of the detectors based on this material [4]. On the other hand, InSb IR detectors are limited by the cryogenic cooling to reduce the thermally generated dark current, which rises the overall system size and cost [5].

InAs/GaSb material system is characterised by a type-II broken gap band line-up where the InAs conduction band minimum is located lower than the top of the GaSb valence band [1]. Therefore, the fundamental transition between the conduction band bottom and the heavy hole sub-bands is determined by the InAs and GaSb layer thickness [6]. This alignment contributes to a reduction of the Auger generation-recombination rate due to the suppression of some non-radiative pathways in the valence band [7]. Besides, the band-to-band tunnelling is significantly reduced due to high electrons and holes effective masses [8].

InAs/GaSb T2SL is commonly deposited on expensive and available in small sizes (less than 3 in) lattice-matched GaSb substrates. Moreover, GaSb substrates are not “epi-ready”, i.e.: they need to be treated (chemically or physically) before the epitaxial deposition. Moreover, their surfaces contain many macroscopic defects [9]. The GaSb absorption coefficient is fairly high assuming $\sim 100 \text{ cm}^{-1}$ for IR range $> 5 \mu\text{m}$ [10]. Due to its many advantages, GaAs was proposed as a feasible substrate candidate for InAs/GaSb T2SL deposition being “epi-ready”, cost-efficient, and available up to 6 in [11–14]. In addition, the GaAs absorption coefficient is two orders of magnitude lower than that of GaSb but a ~7.6% lattice-mismatch between GaAs and InAs/GaSb T2SL contributes to the level of $\sim 10^9 \text{ cm}^{-2}$ misfit dislocation density [15]. There is a need to develop growth conditions to mitigate strain and reduce dislocation densities. The low-temperature nucleation [16], and the interfacial misfit array (IMF) technique [17, 18] have been introduced and implemented to date.

The growth temperature is a very important deposition parameter determining the InAs/GaSb T2SL quality. It is responsible for the surface atoms diffusion and the intermixing of elements between different layers. These phenomena directly affect the crystalline and optical parameters of the T2SL. Consequently, the growth temperature should be high enough to remove the remedies of the group V atoms, and sufficiently low to regulate the

*Corresponding author at: piotr.martyniuk@wat.edu.pl<https://doi.org/10.24425/opelre.2023.144557>

1896-3757/ Association of Polish Electrical Engineers (SEP) and Polish Academic of Sciences (PAS). Published by PAS

© 2023 The Author(s). This is an open access article under the CC BY license (<http://creativecommons.org/licenses/by/4.0/>).

atoms intermixing at different interfaces. Generally, the InAs/GaSb T2SL deposition temperatures reported by previous groups are 400 ± 10 °C [19–25]. However, there are some groups which reported a growth temperature of 420 °C [26, 27] and 430 °C [28].

This paper presents the InAs/GaSb T2SLs molecular beam epitaxy (MBE) growth conditions on the $\sim 7.6\%$ lattice-mismatched GaAs (001), 2° offcut towards $\langle 110 \rangle$ substrates. This deposition is conducted at lower temperatures in comparison to those mentioned previously.

2. Experiment

Several 30 period (P) 10 monolayers (ML) InAs/10ML GaSb T2SLs were grown on GaAs (001), 2° offcut towards $\langle 110 \rangle$ substrates at selected low temperatures. Samples were deposited by a RIBER Compact 21-DZ MBE system. The MBE was equipped with gallium (Ga) and indium (In) standard effusion cells and with arsenic (As) and antimony (Sb) valved cracked cells. The substrate temperature was monitored by a manipulator thermocouple.

First, the deoxidization of the GaAs substrate at 625 °C was conducted. Later, a 0.6 μm thick GaAs buffer layer was deposited at 590 °C in order to get a smooth surface. Then, a 1.5 μm thick GaSb layer was deposited at 465 °C to mitigate the lattice-mismatch between the GaAs substrate and T2SLs. The growth conditions of a GaSb buffer are reported elsewhere [29]. Later, 30 P 10ML InAs/10ML GaSb T2SLs were deposited at several growth temperatures: 330, 350, and 370 °C. The V/III flux ratio was assumed at a level of 8.3 and 4.6 for InAs and GaSb, respectively. The growth rate was 0.33 $\mu\text{m}/\text{h}$ and 0.76 $\mu\text{m}/\text{h}$ for InAs and GaSb, respectively. In order to mitigate the strain between InAs and GaSb, the shutters sequence presented in Fig. 1 was used. The InAs deposition was followed by 8 s Sb soak to form InSb-like bonds. The GaSb deposition was followed by a 2 s As soak to grow a GaAs-like interface. The deposition was controlled *in situ* by a reflection high-energy electron diffraction system (RHEED).

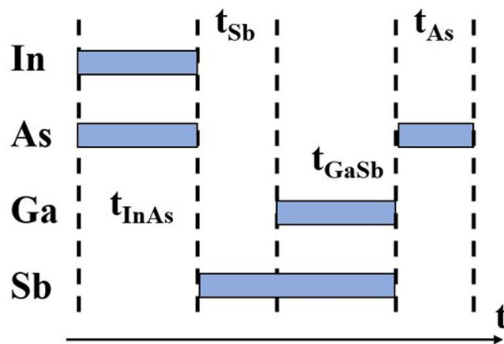


Fig. 1. The shutter sequence for the InAs/GaSb T2SLs growth.

The surface roughness was quantitatively evaluated by a high-resolution optical profilometer. A PANalytical X'Pert high-resolution X-ray diffractometer (HRXRD) was used to determine the InAs/GaSb T2SLs structural properties. The Cu $K_{\alpha 1}$ $\lambda \approx 1.5406$ Å was used and X-ray beam was monochromatized by a four-bounce Ge (004) hybrid monochromator. The measurements were performed in a 2θ - ω direction. The electrical properties were assessed by the Hall effect measurements based on the Van de Pauw method. Spectral responsivity has been

measured by a Fourier transform infrared (FTIR) spectrophotometer.

3. Results and discussions

The T2SLs InAs/GaSb surface morphology/surface roughness (Rq), full width at half maximum (FWHM), and lattice-mismatch GaAs-zero-order/GaSb ($\Delta a/a$) are presented in Table 1. As can be seen, three samples exhibit practically the same Rq . On the other hand, the InAs/GaSb T2SLs grown at 330 °C exhibit the best structural parameter, with a FWHM of 103 arcsec. That characterisation data proves the high quality of T2SLs (grown at low temperatures). This is probably due to the reduction of the dislocation density at low temperatures. It should be noted that the dislocation density at the GaSb-GaAs interface substrate has been determined to be as low as 10^8 cm^{-2} [18].

Figure 2 presents the high-resolution XRD pattern around the symmetric 004 reflection of a 30 P 10ML InAs/10ML GaSb T2SL grown on GaAs substrates. There are two peaks from the GaAs ($2\theta = 66.07^\circ$) substrate and the GaSb ($2\theta = 60.73^\circ$) buffer layer, in addition to the satellite peaks visible up to the third order (shown as “0”, “ ± 1 ”). This is the evidence of the good crystalline quality and the high reproducibility of the InAs/GaSb T2SLs. The FWHMs of the zero-order peaks are reported in Table 1.

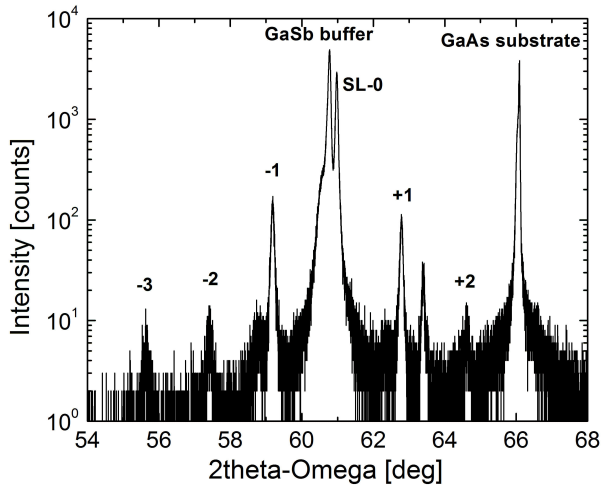
Table 1.
Structural parameters of InAs/GaSb T2SL vs. the growth temperature.

T [°C]	Rq [nm]	FWHM [arcsec]	$\Delta a/a$ [%]
370	7.8	150	-0.94
350	7.3	107	-0.89
330	7.1	103	-0.87

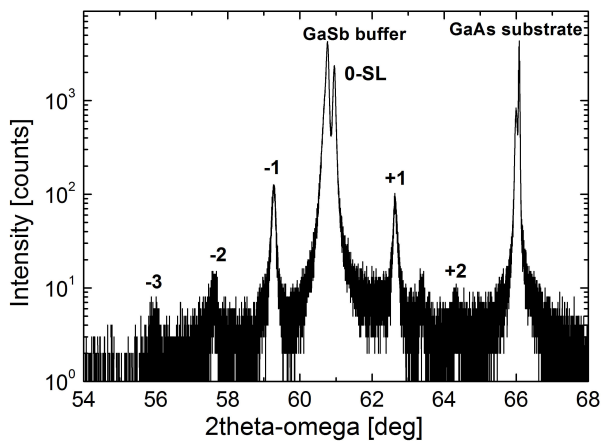
It should be noted that there were other growths at high temperature conditions, but T2SLs were not observed. This is due to the desorption of the atoms from the surface. Figure 3 shows that there are no satellite peaks indicating the lack of T2SLs. Only the presence of the GaAs and GaSb peaks can be seen. Besides, satellites were not present in the samples grown at a temperature below 330 °C.

Figure 4 presents the Hall concentration of the grown InAs/GaSb T2SLs. The samples deposited at 350 °C exhibit a change of conductivity at 145 K. It has n-type conductivity at high temperature, and p-type at low temperature. This result was reported by several groups previously [8, 30]. This is due to different types of impurities at low and high temperatures. Besides, other two samples grown at 330 and 370 °C are characterised by n-type and p-type, respectively. This can be seen in the trend of both curves. This unique conductivity dependence is probably due to the creation of one dominant level of impurities during the low growth temperature.

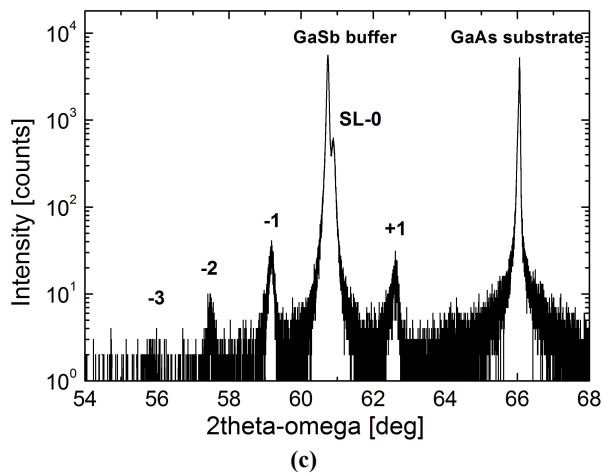
Figure 5 illustrates the spectral responsivity of the grown sample at a temperature of 330 °C, measured at 230 and 300 K. As can be seen, the InAs/GaSb T2SLs present a 50% cut-off wavelength of 5.4 μm , which is located in the mid-wave IR (MWIR) region. It should be noted that the sample exhibits a spectral response despite the small thickness of the T2SLs (only 30 P).



(a)



(b)



(c)

Fig. 2. (004) HRXRD 2θ-ω scan for the 30 P InAs/GaSb T2SLs deposited at 330 °C (a), 350 °C (b), and 370 °C (c).

4. Conclusions

The InAs/GaSb T2SLs have been deposited at relatively low temperature on a GaAs substrate with 2° offcut towards <110>. The grown layers exhibit a good surface morphology or a shiny mirror-like surface. Despite the ~7.6% lattice-mismatch between GaAs and InAs/GaSb T2SLs, comparable crystalline quality and Rq to that of

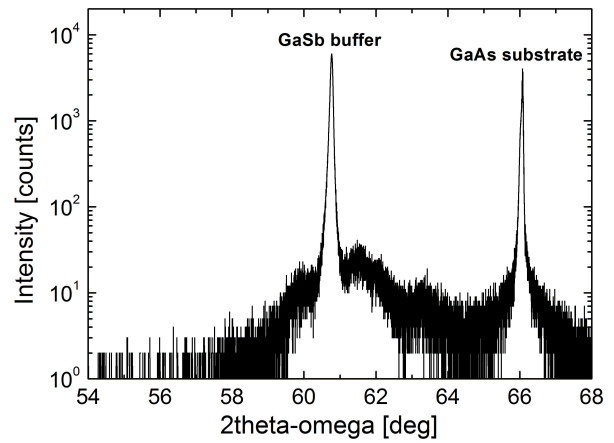


Fig. 3. (004) HRXRD 2θ-ω scan for the InAs/GaSb T2SL deposited at $T > 370$ °C.

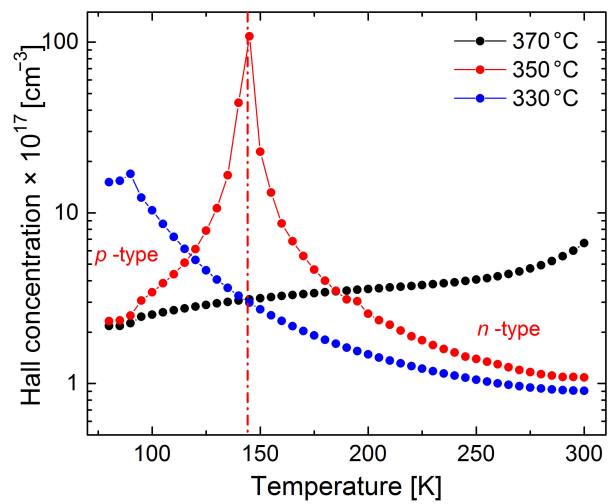


Fig. 4. Hall concentration of three deposited InAs/GaSb T2SLs.

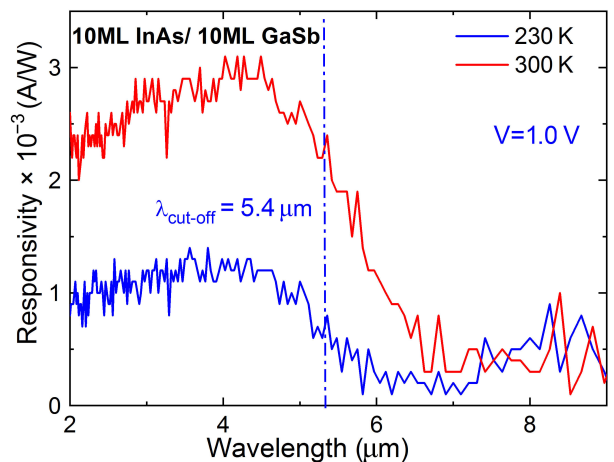


Fig. 5. Spectral responsivity of the InAs/GaSb T2SLs grown at 330 °C.

T2SLs deposited on GaSb were achieved. The electrical parameters are found to be dependent on the deposition temperature. The InAs/GaSb T2SLs can present n-type or p-type conductivity or even both. This important characteristic can be used in the conception of IR detectors or transistors.

Acknowledgements

This paper was supported by Polish National Science Centre: 2018/31/B/ST7/01541 and 2018/30/M/ST7/00174.

References

- [1] Sai-Halasz, G. A., Tsu, R. & Esaki, L. A new semiconductor superlattice. *Appl. Phys. Lett.* **30**, 651–653 (1977). <https://doi.org/10.1063/1.89273>
- [2] Razeghi, M. *et al.* State-of-the-art type II antimonide-based superlattice photodiodes for infrared detection and imaging. *Proc. SPIE* **7467**, 74670T (2009). <https://doi.org/10.1117/12.828421>
- [3] Plis, E. A. InAs/GaSb type-II superlattice detectors. *Adv. Electron.* **2014**, 1–12 (2014). <https://doi.org/10.1155/2014/246769>
- [4] Li, Q. *et al.* SRH suppressed P-G-I design for very long-wavelength infrared HgCdTe photodiodes. *Opt. Express* **30**, 16509–16517 (2022). <https://doi.org/10.1364/OE.458419>
- [5] Wang, F. *et al.* Fully depleted self-aligned heterosandwiched Van Der Waals photodetectors. *Adv. Mater.* **34**, 2203283 (2022). <https://doi.org/10.1002/adma.202203283>
- [6] Rodriguez, J. B., Christol, P., Cerutti, L. & Chevrier, F. MBE growth and characterisation of type-II InAs/GaSb superlattices for mid-infrared detection. *J. Cryst. Growth* **274**, 6–13 (2005). <https://doi.org/10.1016/j.jcrysgro.2004.09.088>
- [7] Grein, C. H., Cruz, H., Flatté, M. E. & Ehrenreich, H. Theoretical performance of very long wavelength InAs/In_xGa_{1-x}Sb superlattice based infrared detectors. *Appl. Phys. Lett.* **65**, 2530–2532 (1994). <https://doi.org/10.1063/1.112626>
- [8] Mohseni, H., Litvinov, V. I. & Razeghi, M. Interface-induced suppression of the Auger recombination in type-II InAs/GaSb superlattices. *Phys. Rev. B* **58**, 15378–15380 (1998). <https://doi.org/10.1103/PhysRevB.58.15378>
- [9] Plis, E. *et al.* Mid-infrared InAs/GaSb strained layer superlattice detectors with nBn design grown on a GaAs substrate. *Semicond. Sci. Technol.* **25**, 085010 (2010). <https://doi.org/10.1088/0268-1242/25/8/085010>
- [10] Chandola, A., Pino, R. & Dutta, P. S. Below bandgap optical absorption in tellurium-doped GaSb. *Semicond. Sci. Technol.* **20**, 886–893 (2005). <https://doi.org/10.1088/0268-1242/20/8/046>
- [11] Bao, T. *et al.* GaAs Based InAs/GaSb superlattice short wavelength infrared detectors grown by molecular beam epitaxy *Chinese Phys. Lett.* **26**, 028102 (2009). <https://doi.org/10.1088/0256-307X/26/2/028102>
- [12] Nguyen, B.-M. *et al.* Demonstration of midinfrared type-II InAs/GaSb superlattice photodiodes grown on GaAs substrate. *Appl. Phys. Lett.* **94**, 223506 (2009). <https://doi.org/10.1063/1.3148326>
- [13] Zhang, X. B., Ryou, J. H. & Dupuis, R. D. Metalorganic chemical vapor deposition growth of high-quality InAs/GaSb type II superlattices on (001) GaAs substrates. *Appl. Phys. Lett.* **88**, 072104(2006). <https://doi.org/10.1063/1.2168668>
- [14] Benyahia, D. *et al.* Comparative study of the molecular beam epitaxial growth of InAs/GaSb superlattices on GaAs and GaSb substrates. *Acta Phys. Pol. A* **132**, 322–324 (2017). <https://doi.org/10.12693/APhysPolA.132.322>
- [15] Johnson, G. R., Cavenette, B. C., Kerr, T. M., Kirby, B. P. & Wood, C. E. C. Optical, Hall and cyclotron resonance measurements of GaSb grown by molecular beam epitaxy. *Semicond. Sci. Technol.* **3**, 1157 (1988). <https://doi.org/10.1088/0268-1242/3/12/002>
- [16] Michel, E., Mohseni, H., Kim, J. D. & Wojtkowski, J. High carrier lifetime InSb grown on GaAs substrates. *Appl. Phys. Lett.* **71**, 1071–1073 (1997). <https://doi.org/10.1063/1.119731>
- [17] Huang, H. S. *et al.* Strain relief by periodic misfit arrays for low defect density GaSb on GaAs. *Appl. Phys. Lett.* **88**, 131911 (2006). <https://doi.org/10.1063/1.2172742>
- [18] Benyahia, D. *et al.* Interfacial misfit array technique for GaSb Growth on GaAs (001) substrate by molecular beam epitaxy. *J. Electron. Mater.* **47**, 299–304 (2018). <https://doi.org/10.1007/s11664-017-5766-4>
- [19] Schmitz, J. *et al.* Optical and structural investigations of intermixing reactions at the interfaces of InAs/AlSb and InAs/GaSb quantum wells grown by molecular-beam epitaxy. *J. Cryst. Growth* **150**, 858–862 (1995). [https://doi.org/10.1016/0022-0248\(95\)80061-G](https://doi.org/10.1016/0022-0248(95)80061-G)
- [20] Fuchs, F. *et al.* InAs/Ga_{1-x}In_xSb infrared superlattice photodiodes for infrared detection. *Proc. SPIE* **3287**, 14–22 (1998). <https://doi.org/10.1117/12.304477>
- [21] Haugan, H. J., Szmilowicz, F., Mahalingam, K. & Brown, G. J. Optimization of mid-infrared InAs/GaSb type-II superlattices. *Appl. Phys. Lett.* **84**, 5410–5412 (2004). <https://doi.org/10.1063/1.1767598>
- [22] Sullivan, G. J., Ikhlassi, A., Bergman, J., DeWames, R. E. & Waldrop, J. R. Molecular beam epitaxy growth of high quantum efficiency InAs/GaSb superlattice detectors. *J. Vac. Sci. Technol. B* **23**, 1144–1148 (2005). <https://doi.org/10.1116/1.1928238>
- [23] Sankowska, I. *et al.* Non-periodicity of peak-to-peak distances in x-ray diffraction spectrums from perfect superlattices. *J. Appl. Phys.* **113**, 064302 (2013). <https://doi.org/10.1063/1.4790712>
- [24] Wei, Y., Gin, A. & Razeghi, M. Advanced InAs/GaSb superlattice photovoltaic detectors for very long wavelength infrared applications. *Appl. Phys. Lett.* **80**, 3262–3264 (2002). <https://doi.org/10.1063/1.1476395>
- [25] Kaspia, R., Steinshneider, J., Weimer, M., Moeller, C. & Ongstad, A. As-soak control of the InAs-on-GaSb interface. *J. Cryst. Growth* **225**, 544–549 (2001). [https://doi.org/10.1016/S0022-0248\(01\)00950-2](https://doi.org/10.1016/S0022-0248(01)00950-2)
- [26] Plis, E. *et al.* Type-II InAs/GaSb strained layer superlattices grown on GaSb (111) B substrate. *J. Vac. Sci. Technol. B* **31**, 03C123 (2013). <https://doi.org/10.1116/1.4798650>
- [27] Wang, G.-W. *et al.* Growth and characterisation of GaSb-Based type-II InAs/GaSb superlattice photodiodes for mid-infrared detection. *Chinese Phys. Lett.* **27**, 077305 (2010). <https://doi.org/10.1088/0256-307X/27/7/077305>
- [28] Renard, C. *et al.* Indium surface segregation in AlSb and GaSb. *J. Cryst. Growth* **259**, 69–78 (2003). <https://doi.org/10.1016/j.jcrysgro.2003.07.010>
- [29] Benyahia, D. *et al.* Low-temperature growth of GaSb epilayers on GaAs (001) by molecular beam epitaxy. *Opto-Electron. Rev.* **24**, (2016). <https://doi.org/10.1515/oere-2016-0007>
- [30] Khoshakhlagh, A. *et al.* Background carrier concentration in midwave and longwave InAs/GaSb type II superlattices on GaAs substrate. *Appl. Phys. Lett.* **97**, 051109 (2010). <https://doi.org/10.1063/1.3457908>